Single-cell transcriptome profiling implicates the psychological stress-induced disruption of spermatogenesis

Rufeng Li,[1,5] Yuefeng Du,[2,5] Kang Li,[1] Xiaofan Xiong,[3] Lingyu Zhang,[1] Chen Guo,[1] Shanfeng Gao,[1] Yufei Yao,[1] Yungang Xu,[1] and Juan Yang[1,4]

[1]Department of Cell Biology and Genetics, School of Basic Medical Sciences, Xi'an Jiaotong University Health Science Center, Xi'an 710061, P.R. China; [2]Department of Urology, the First Affiliated Hospital of Xi'an Jiaotong University, Xi'an 710061, P.R. China; [3]Center for Tumor and Immunology, the Precision Medical Institute, the Second Affiliated Hospital of Xi'an Jiaotong University, Xi'an 710004, P.R. China; [4]Key Laboratory of Environment and Genes Related to Diseases (Xi'an Jiaotong University), Ministry of Education of China, Xi'an 710061, P.R. China

Male infertility has emerged as a global issue, partly attributed to psychological stress. However, the cellular and molecular mechanisms underlying the adverse effects of psychological stress on male reproductive function remain elusive. We created a psychologically stressed model using terrified-sound and profiled the testes from stressed and control rats using single-cell RNA sequencing. Comparative and comprehensive transcriptome analyses of 11,744 testicular cells depicted the cellular landscape of spermatogenesis and revealed significant molecular alterations of spermatogenesis suffering from psychological stress. At the cellular level, stressed rats exhibited delayed spermatogenesis at the spermatogonia and pachytene phases, resulting in reduced sperm production. Additionally, psychological stress rewired cellular interactions among germ cells, negatively impacting reproductive development. Molecularly, we observed the down-regulation of anti-oxidation-related genes and up-regulation of genes promoting reactive oxygen species (ROS) generation in the stress group. These alterations led to elevated ROS levels in testes, affecting the expression of key regulators such as ATF2 and STAR, which caused reproductive damage through apoptosis or inhibition of testosterone synthesis. Overall, our study aimed to uncover the cellular and molecular mechanisms by which psychological stress disrupts spermatogenesis, offering insights into the mechanisms of psychological stress-induced male infertility in other species and promises in potential therapeutic targets.

INTRODUCTION

Male infertility is a common condition that affects at least 7% of men worldwide and is on the rise.[1] Moreover, male infertility is the sole factor in 20%–30% of infertility cases, but the pathogenesis of 70% of male infertility cases remains unclear.[2] Currently, numerous studies have shown that stress is an important factor affecting the physical and mental state of healthy individuals and can disturb the internal homeostasis of the body. With the development of society and the increase of competitive pressure in all aspects of life, long-term stress can affect the physiological functions of the human body, including adverse effects on metabolism, immune function, the nervous system, the cardiovascular system, and the reproductive system, leading to disease.[3,4] Psychological stress has also emerged as one of the important potential risk factors affecting male fertility.[4–7] It has been reported that severe physical and psychological stress under the stimulation of external factors can cause a decrease in the quality of gonads such as prostate, seminal vesicles, testes, and epididymis, as well as a disturbance in the secretion of sex hormone levels. This impaired the function of the male gonadal axis, resulting in abnormal sperm production and decreased quality.[8] Psychological stress may also lead to significantly lower plasma testosterone (T) levels,[9,10] thereby reducing sperm count and motility.[11] In addition, studies have shown that the sperm quality of patients with male infertility caused by psychological stress improved significantly after psychotherapy, indicating that psychological stress is an important factor contributing to male infertility,[12,13] but the mechanisms involved have not been thoroughly described.

The development of single-cell omics has greatly facilitated the exploration of specific mechanisms in male infertility. As one of the key technologies in single-cell omics research, single-cell transcriptome sequencing is currently widely used. Since Tang et al.[14] completed the first single-cell RNA sequencing (scRNA-seq) in 2009, scRNA-seq has been continuously improved and has become a common method for whole-cell expression analysis with the emergence of
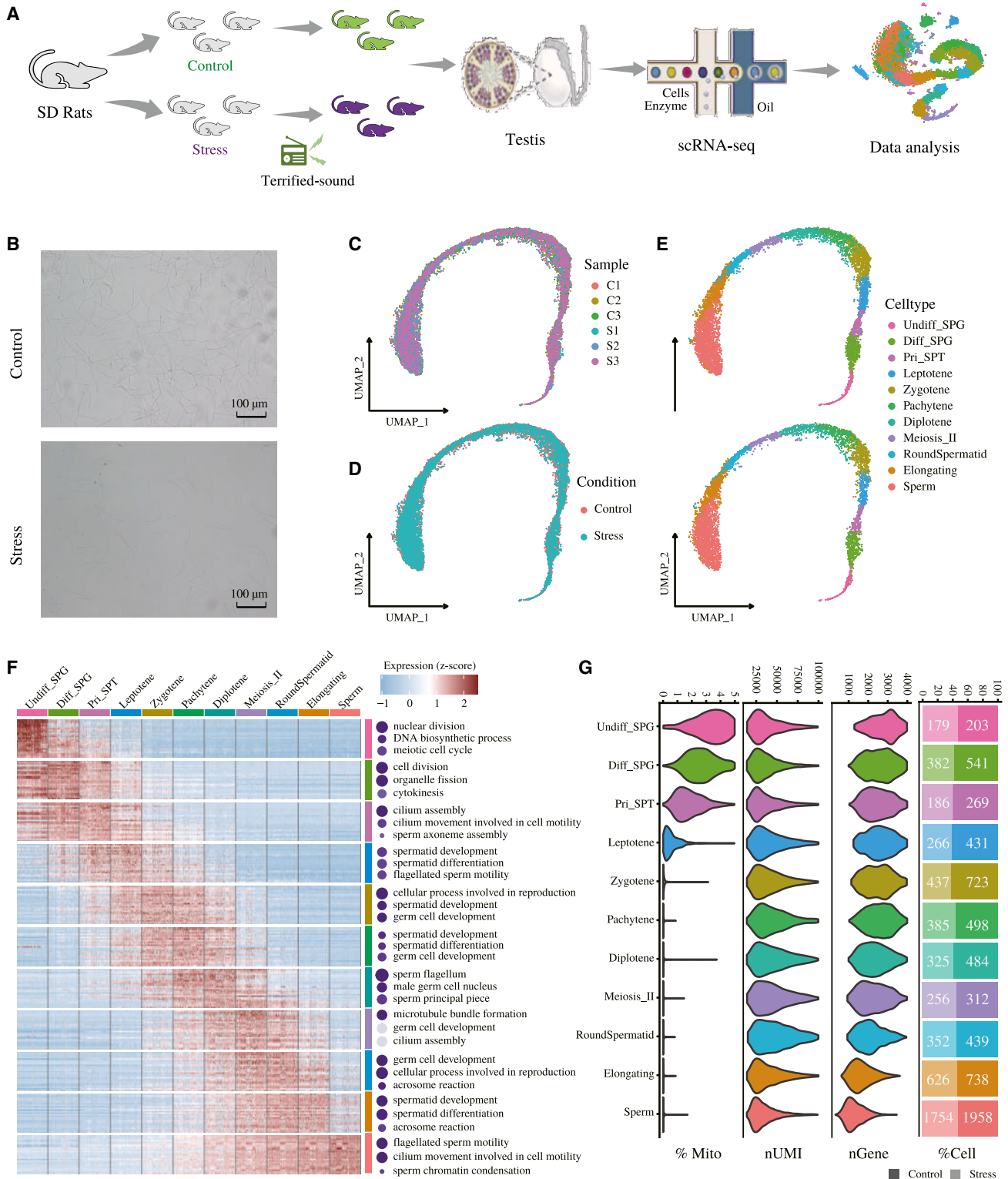
Figure 1. The single-cell atlas for spermatogenesis of rats

(A) The schematic view of the experimental workflow. (B) Temporary slide microscopy shows lower sperm count in the caudal epididymis of psychologically stressed rats compared with controls. (C) The UMAP plot shows testicular cell distributions of the normal and stressed rats (n = 3 for each group). Each dot represents a testicular cell and is

(legend continued on next page)

some large commercial platforms.[15] Over the past decade, scRNA-seq has also been widely used to study gene expression patterns of spermatogenesis and to reveal the dynamic process and key regulatory factors of spermatogenesis, which produces mature male gametes.[16–20] Especially, single-cell resolved transcriptome profiling can greatly promote the exploration of the specific effects of chronic psychological stress on the complex process of spermatogenesis.

Furthermore, animal studies have shown that psychological stress can disrupt the function of the hypothalamic-pituitary-testis axis by reducing the release of luteinizing hormone and follicle-stimulating hormone (FSH),[21,22] resulting in testicular cell apoptotic death.[23] Our previous study also revealed that male rats exposed to psychological stress showed slow growth, reduced sperm quality, and abnormal levels of reproductive endocrine hormones.[24] Understanding the effects of psychological stress on the infertility of animal models can provide strong support for the discovery of similar mechanisms in humans. Therefore, in this work, we used our previously created terrified-sound stressed model in Sprague-Dawley (SD) rats (*Rattus norvegicus*)[24] and performed scRNA-seq of the testicular tissues from the stressed and normal rats (Figure 1A). Through the comparative and comprehensive analyses of the transcriptomes of the two groups, we revealed the specific mechanism by which the psychological stress of terrified-sound affects the process of spermatogenesis and ultimately leads to reproductive damage in male rats. The findings provide a theoretical basis for the study of psychological stress on male reproductive impairments for other animals and humans, and further promise in finding therapeutic targets for male infertility caused by psychological stress.

RESULTS

Single-cell transcriptomics delineates the cellular landscape of spermatogenesis

To investigate the effect of terrified-sound psychological stress on reproductive damage in male rats, we constructed a model of terrified-sound psychological stress with male SD rats. Histologically, we observed (by H&E staining) a reduction in the number of germ cells in the testes of rats subjected to terrified-sound psychological stress (Figure S1A). The sperm density was also decreased in rats in the stress group (Figure 1B). To further explore the effect of terrified-sound on the testis of male rats, we performed scRNA-seq on testicular tissues from three control and three terrified-sound-stressed male rats, respectively (Figure 1A). A total of 9,000 and 8,998 cells for the control group and the stress group, respectively, were captured from the raw data. After quality control (see materials and methods for details), 11,744 cells (6,596 cells from the control group and 5,148 cells from the stress group) (Table S1) and 23,170 genes were retained for subsequent analyses. Next, we calculated the cell cycle score for each cell. Principal-component analysis (PCA) plots show a good overlap between different periods (Figure S2A). UMAP plots show that different cell types contain various periods of the cell cycle (Figure S2B). These findings indicate that our data have a lower cell cycle dependency. Therefore, our subsequent analysis was not corrected for cell cycle effects. After batch correction with Harmony[25] (Figures 1C and 1D), we built the cell atlas of rat spermatogenesis with 11 cell clusters using unsupervised clustering. To assign identities to the clusters, we determined the expression of known cell-type-specific marker genomes and identified 11 germ cells at various stages (Figures 1D and 1E), covering the sperm differentiation progression: Undifferentiated spermatogonia (Undiff_SPG), differentiated spermatogonia (Diff_SPG), primary spermatocytes (Pri_SPT), leptotene, zygotene, pachytene, diplotene, second secondary meiotic cells (Meiosis_II), round sperm cells (RoundSpermatid), elongated sperm cells (Elongating), and sperm cells. We confirmed the correct clustering assignment by evaluating the expression of specific marker genes (Figure S2C; Table S2). Furthermore, we performed Gene Ontology (GO) enrichment of the marker genes for each cell cluster, which further confirmed the assigned cell types (Figure 1F). In addition, we further examined the distribution of cell types in each sample and quantified their relative proportions at different stages of spermatogenesis (Figure S1E).

To characterize our cellular atlas, we show the proportion of mitochondrial-encoded RNA, the total number of genes detected, the total number of unique transcripts, and the proportion of cells from control vs. stress in each cell type (Figure 1G). During spermatogenesis, mitochondria undergo significant changes in morphology, size, localization, and number. Most of the mitochondrial DNA of male germ cells is eliminated during spermatogenesis, and mitochondrial DNA is reduced to one-tenth of its initial number.[26] It has been reported that the reduction of mitochondrial DNA copy number in sperm may reduce the frequency of mitochondrial DNA damage. We found that mitochondrial mRNA levels gradually decreased with the spermatogenesis process. In particular, the mitochondrial mRNA level decreased significantly after entering meiosis. This is consistent with previous reports. Furthermore, the total number of genes detected, as well as the total number of unique transcripts, did not vary significantly across most cell types. But these are reduced in sperm cells compared with other cells.

Psychological stress induces cell-type-specific transcriptomic alterations during spermatogenesis

To understand how psychological stress with terrified-sound will affect the transcriptome rat germ cells, we performed differential expression analysis and functional enrichment analysis for each cell type during spermatogenesis (Figure S3; Table S3). We found that

colored according to its sample source, wherein C1–C3 refers to three rats from the control group, and S1–S3 refers to the three rats from the stressed group. (D) The UMAP plot shows testicular cell distributions of the normal and stressed rats (n = 3 for each group). Each dot represents a testicular cell and is colored according to its group source. (E) The UMAP plots show the 11 clusters with annotated cell types for normal (n = 3) and stressed (n = 3) rats, respectively. Each dot represents a testicular cell and is colored according to its cell type. (F) The top 25 differentially expressed genes and their enriched GO terms for each cell cluster. (G) Comparison of distribution profiles for each cell attribute across 11 cell types.
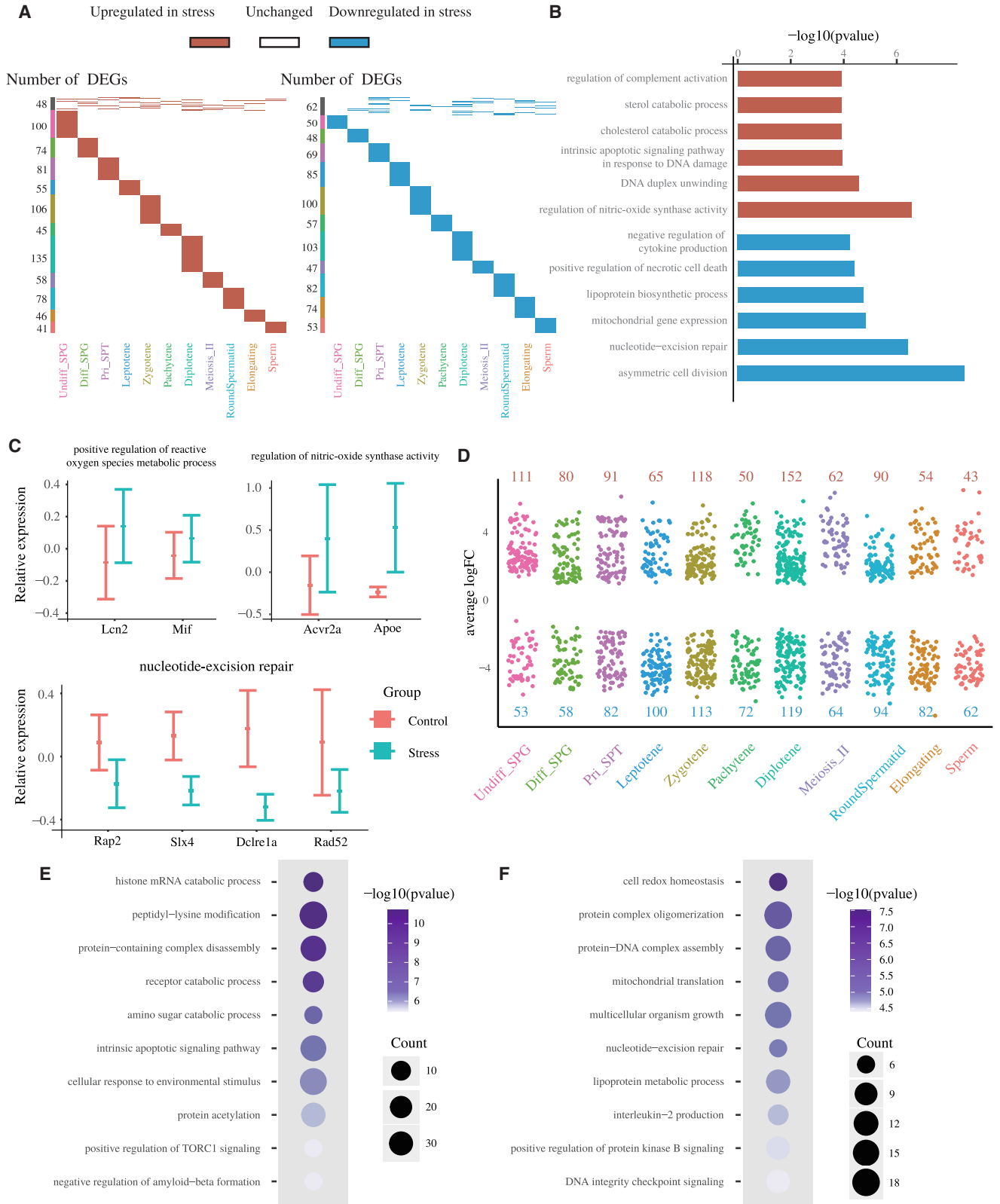
(legend on next page)

most differentially expressed genes (DEGs) are specific to a single cell type (819 up-regulated genes and 768 down-regulated genes), indicating the cell-type-specific effects of psychological stress. In addition, there are also many DEGs (both the up- and down-regulated genes) that are shared across multiple cell types, including 48 up-regulated genes and 62 down-regulated genes shared by at least two cell types. Functional enrichment analysis of the commonly up-regulated genes revealed significant changes in reactive oxygen species (ROS)-related processes, including "regulation of nitric-oxide synthase activity," "positive regulation of ROS metabolic process," etc. (Figure 2B). A list of representative ROS genes shows significant up-regulation after psychological stress (Figure 2C), including Lcn2 (lipocalin 2) and Mif (macrophage migration inhibitory factor), which are related to ROS metabolism, and Acvr2a (activin A receptor type 2A), Apoe (apolipoprotein E), which are related to nitric oxide (NO) synthesis.[27,28] Notably, in addition to the up-regulated ROS genes in the stress group, we also found ROS scavenging-related genes such as Gstp1, Gsr, etc.[29] were down-regulated in the stress group. These results imply that external psychological stress may cause excessively elevated ROS levels in the testes of rats to further induce intracellular oxidative stress (OS). Numerous previous studies have shown that OS will reduce fertility through lipid peroxidation, sperm DNA damage, and apoptosis.[30–32] Intriguingly, we also found that the commonly up-regulated genes were enriched in DNA damage-related processes such as "intrinsic apoptotic signaling pathway in response to DNA damage."

Moreover, we also investigated those cell-specific DEGs (Figure 2D). GO enrichment analyses were performed on all up-regulated and down-regulated DEGs, respectively (Figures 2E and 2F). Correspondingly, we noticed DNA damage repair-related enrichments such as "nucleotide-excision repair" in the stressed group, wherein some important genes (Rap2, Slx4, Dclre1a, and Rad52) were significantly down-regulated after psychological stress (Figure 2C). Altogether, the psychological stress of terrified-sound may cause enhanced ROS generation ability and weakened the scavenging ability of rat testis. This leads to OS, which in turn affects some biochemical reactions during spermatogenesis, such as DNA damage repair, apoptosis, etc.

Psychological stress disrupts the cellular dynamics of spermatogenesis

To further reveal the stress-induced effects on cellular transitions during the course of rat spermatogenesis, we investigated the transient cellular dynamics by RNA velocity analysis. We set undifferentiated spermatogonia (Undiff_SPG) as the starting point of spermatogenesis. The velocity streamlines show that spermatogenesis in the control samples starts from Undiff_SPG cells and then directs to differentiated spermatogonia (Diff_SPG), primary spermatocytes

(Pri_SPT), leptotene, zygotene, pachytene, diplotene, second meiotic cells (Meiosis_II), round spermatids (RoundSpermatid), elongated spermatids (Elongating), and finally to spermatids. In contrast, for the stressed group, we observed apparent differentiation arrest during the differentiation of diplotene to pachytene cells (Figure 3A). Besides, latent time suggested that this differentiation arrest may also exist at the transition from spermatogonia to primary spermatocytes (Figure S4A). Additionally, the pseudotime analysis confirmed that the psychological stress retarded the course of spermatogenesis in the stress group as early as in Diff_SPG cells and then the diplotene phase during the differentiation (Figure 3B).

To further evaluate the underlying changes in gene expression throughout spermatogenesis subjected to psychological stress, we performed functional enrichment analysis on the chronologically hypervariable genes over the pseudotime (Figure 3C). Interestingly, we again observed significant enrichments in biological processes related to OS for both groups, such as "cellular response to OS," "response to hydrogen peroxide," etc. Besides, there are some enriched processes related to abiotic stimuli, such as "cellular response to abiotic stimulus" and "cellular response to environmental stimulus." Moreover, changes in some genes with pivotal roles for "chromosome condensation," "protein folding," and "regulation of protein stability" in the stress group may be more helpful to understand the specific mechanism of sperm damage in male rats caused by psychological stress (Figure 3C). Consistent with the group-wise comparisons, the temporally hypervariable genes were also differentially enriched in the biological processes related to ROS between the control and stress groups (Figure S4B). We found that the enrichments of "cellular response to OS," "protein folding," and other related functions in the control group were more significant than that in the stress group. The enrichments of functions such as "cellular response to abiotic stimulus" and "cellular response to environmental stimulus" were more significant in the stress group.

Furthermore, we performed a trajectory-based differential expression analysis of genes specifically enriched in "cellular response to OS" (Figure S4C). We examined the expression of these oxidative stress-related genes over the differentiation course. We found that the expression of genes related to ROS generation, such as Fos and F3, was up-regulated, while the expression of genes encoding antioxidant proteins, such as Hspa8, Nqo1, and Prdx2, was down-regulated. This further points to the fact that psychological stress may retard spermatogenesis by raising ROS in rat testes (Figures 3D, 3E, and S4D).

Psychological stress retards spermatogenesis at the spermatogonia and pachytene phases by elevating ROS

To further explore the phase-specific effects of psychological stress on different segments of spermatogenesis, we divided the course of

---

Figure 2. Transcriptomic alterations of the testicular germ cells

(A) The shared and cell-type-specific DEGs between the control and stressed rats. (B) The enriched GO biological processes of the shared up-regulated (top) or down-regulated (bottom) DEGs between the control and stress groups. (C) The differential expressions of the representative genes for given biological processes. (D) The volcanoplots of the cell-type-specific DEGs after psychological stress. (E) Ten enriched GO terms for up-regulated cell-type-specific DEGs. (F) Ten enriched GO terms for down-regulated cell-type-specific DEGs.
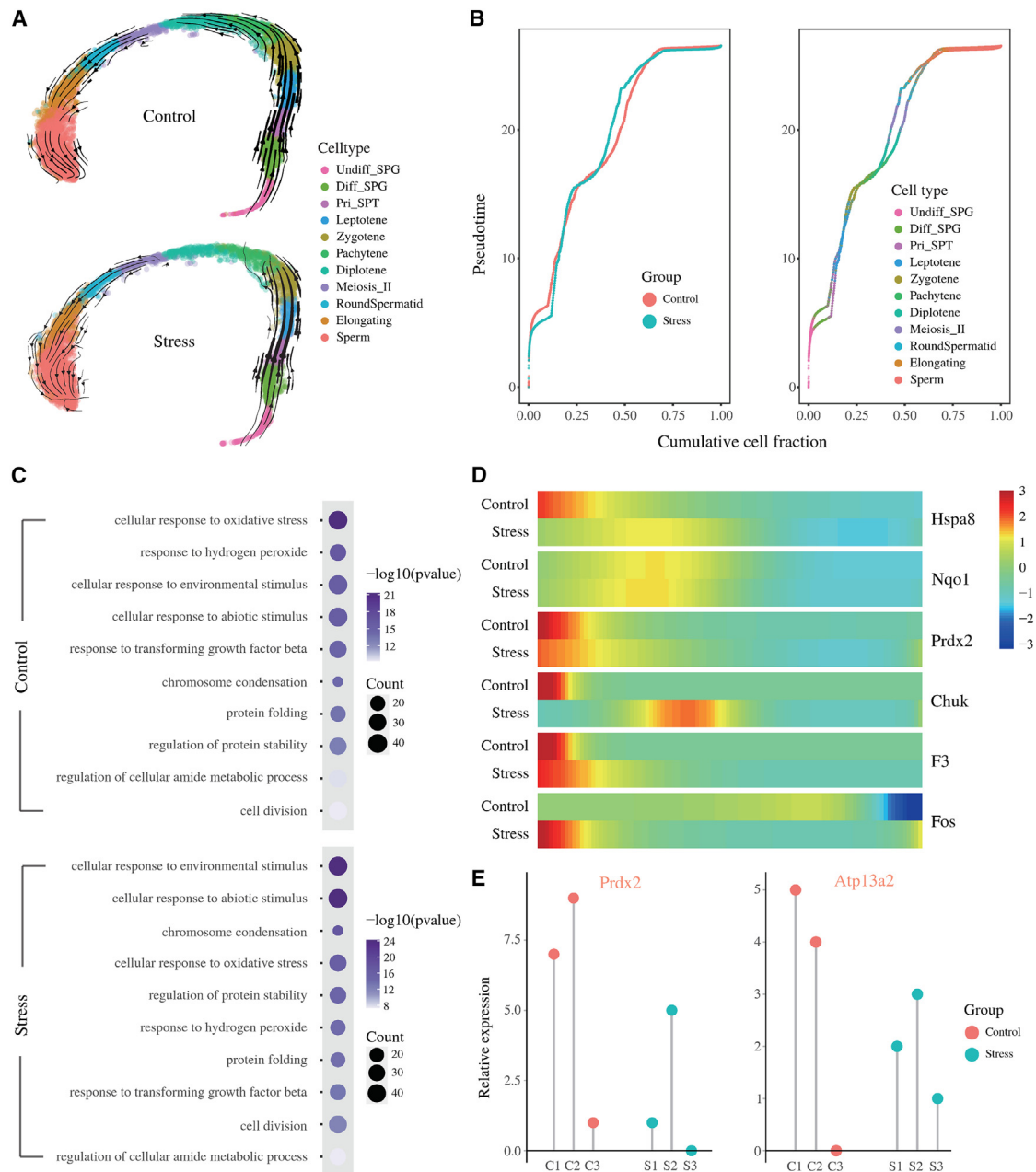
Figure 3. Psychological stress induces spermatogenesis retardations

(A) RNA velocities derived from scVelo kinetic models for normal and stress groups. The streamlines show significant changes between the control and stress groups, indicating spermatogenesis retardation at differentiated spermatogonia and diplotene phase. (B) The cumulative plots of pseudotime highlight spermatogenesis retardations at differentiated spermatogonia and diplotene phases. Each dot represents a cell. (C) The functional enrichment of hypervariable genes for normal and stress groups. (D) Temporal expression of ROS-related genes over differentiation course. (E) Representative ROS genes that are differentially expressed between control and stressed groups.

spermatogenesis into three successive phases: the spermatogonia phase (including Undiff_SPG, Diff_SPG, and Pri_SPT cells), the meiosis phase (including Leptotene, zygotene, pachytene, diplotene, and Meiosis_II cells), and the sperm phase (including RoundSpermatid, Elongating, and Sperm cells). We revisited the

cellular dynamics of each phase in more detail. We first reclustered cells from the spermatogonia phase into more subpopulations and annotated them as "UnSPG.1," "UnSPG.2," "DiSPG.1," "DiSPG.2," "DiSPG.3," "DiSPG.4," and "SPT" (Figures 4A and S5A). RNA velocity analysis revealed "UnSPG.1" as the starting point of the
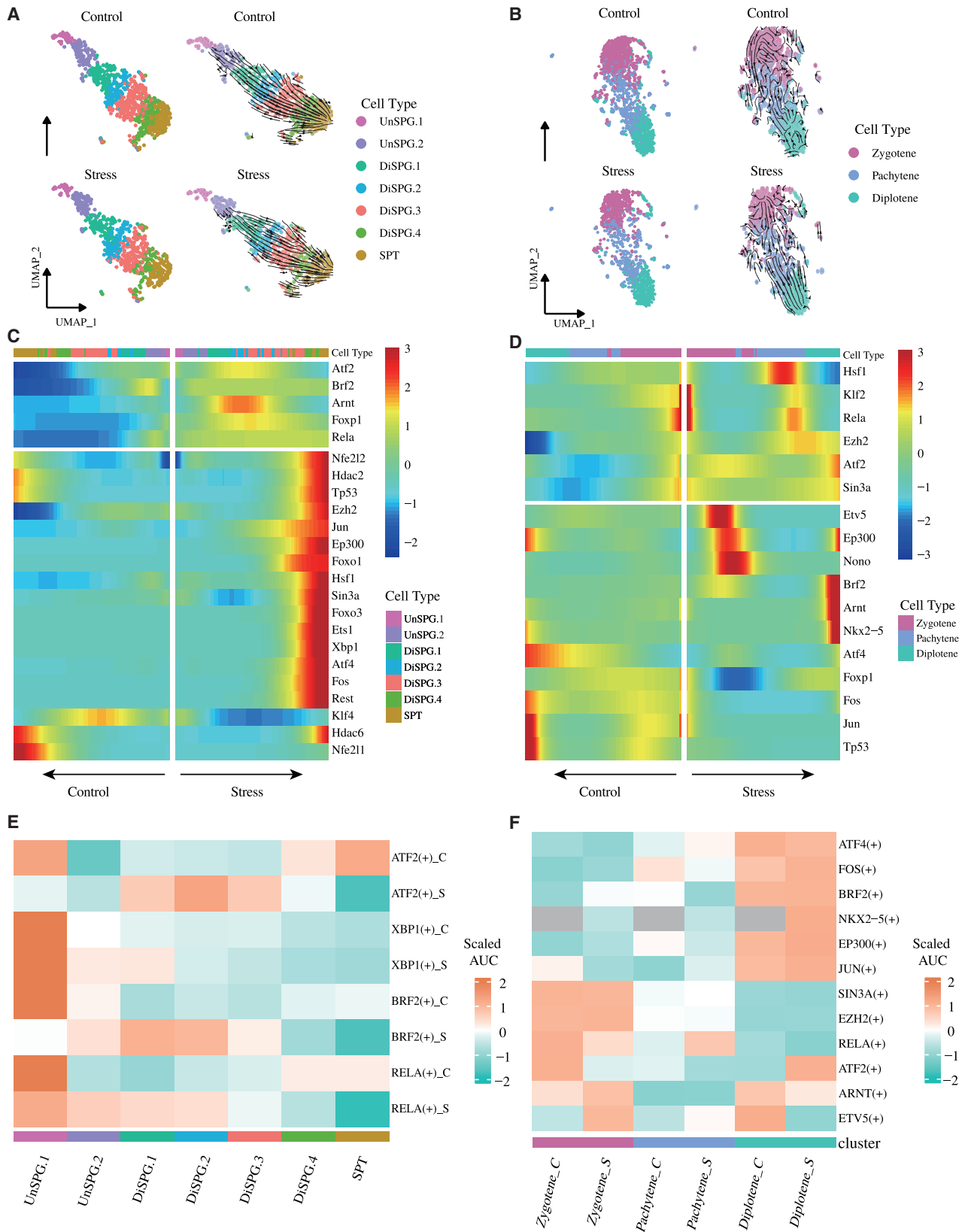
differentiation process. Velocity streamlines indicate that samples in the stress group differ from the control group when "DiSPG.1" points to "DiSPG.2." "DiSPG.1" in the stress group seemed to have more cells flowing toward and into a similar direction to "UnSPG.2" (Figure 4A). We assessed the cellular composition at the spermatogonia phase and found an increased number of cells in "UnSPG.2," "DiSPG.1," "DiSPG.2," and "DiSPG.3" in the stress dataset. However, "UnSPG.1" cells at the beginning of differentiation and "DiSPG.4" at the end of differentiation at the spermatogonia phase, as well as "SPT" cells, were reduced compared with the control dataset (Figure S5B). We speculate that spermatogenesis in male rats after stress is blocked during the differentiation of "DiSPG.1" into "DiSPG.2." Additionally, we performed differential expression analysis for each cell type during the spermatogonia phase (Table S4). Then, we performed gene set enrichment analysis on the DEGs of "DiSPG.1" cells. We found that the "response to hydrogen peroxide" pathway was down-regulated in the stress group (Figure S5C). Notably, HDAC6, GPX1, and STAR genes were all down-regulated in the stress group. Among them, HDAC6 and GPX1 encode antioxidant proteins.[33,34] Their down-regulated expression may be one of the reasons accounting for the excessive ROS caused by psychological stress. Moreover, it is interesting to note that high ROS levels lead to down-regulation of STAR expression, resulting in the inhibition of testosterone synthesis, which in turn leads to reproductive toxicity.[35]

Similarly, we also performed RNA velocity analysis for the meiotic phase, wherein cells from the control group differentiate from "zygotene" to "pachytene", and then from "pachytene" to "diplotene." In the stressed group, the flows of the velocity streamlines were opposite that of the control group (Figure 4B), which indicates that the process of rat spermatogenesis was retarded in meiosis after the psychological stress of terrified-sound. In addition, we also performed the same RNA velocity analysis for the sperm phase. However, no significant difference was observed between the stressed and control groups (Figure S6A).

To further reveal the upstream regulatory basis of the DEGs and the hypervariable genes between the stress and control groups, we used SCENIC to identify "regulons," of which each is a group of genes collectively regulated by a specific transcription factor. Overall, we identified 255 regulons in the two datasets, each containing up to 4,999 genes. We performed functional enrichment analysis on these 255 regulators and found the GO term "cellular response to OS" (Figure S5D). To assess potential changes in gene expression observed during spermatogenesis in stressed samples, we used trajectory-based differential expression analysis. Cells were aligned along the latency time, and cell annotation indicated a sequence of spermatogenesis progression (Figures 4C and 4D). We found that the expression of genes that promote ROS production, such as Fos, were up-regulated during the spermatogonia phase and down-regulated during the meiosis phase in the stressed group.

Furthermore, the results of the SCENIC analysis showed that "DiSPG.1" cells displayed significantly enhanced activation of four regulons in stressed samples: ATF2 (77 genes), XBP1 (20 genes), BRF2 (106 genes), and RELA (71 genes) (Figure 4E). Relatively, the RELA regulon was significantly activated in "pachytene" cells, while the ATF2 and BRF2 regulons were inactivated during the meiosis phase (Figure 4F). Notably, these four regulators did not show this trend in other cell types during the spermatogonia phase. They even exhibit down-regulation of activity during early and late differentiation. Additionally, among the genes regulated by ATF2, we identified RELA. However, other transcription factors do not appear to be mutually regulated. Interestingly, activation of ATF2 regulon was significantly enhanced in "DiSPG.1" cells, but the expression of the gene itself was down-regulated (Figure S6B). According to the reported studies, elevated levels of ROS do lead to a decrease in ATF2 expression. However, ATF2 and its regulated genes act as a regulon, and its increased activity may cause unfavorable spermatogenesis, such as apoptosis.[36–38] Altogether, the above results suggest that psychological stress could cause rat spermatogenesis retardation, specifically at the spermatogonia and pachytene phases, by elevating the ROS.

Psychological stress rewires testicular interactions in a manner detrimental to reproductive development

The process of spermatogenesis is very complex but is highly organized, involving a series of intricate cell-cell interactions between germ cells.[39] We then investigated the cell-cell communications between germ cells to reveal how psychological stress could affect the testicular interactions during spermatogenesis. Compared with the control group, the number and strength of interactions between germ cells in the testes of the stress group showed attenuation (Figure 5A). In particular, compared with the control group, we noticed that the number and strength of interactions between pachytene cells and zygotene, diplotene, and other cells were significantly reduced

Figure 4. Spermatogonia and pachytene retardation in stressed rats
(A) Streamline plot of RNA velocity for the spermatogonia phase. Retardation in streamline flows can be observed in the stress group. (B) Streamline plot of RNA velocity for the meiosis phase. Retardation in streamline flows can be observed in the stress group. (C) Twin heatmaps showing normalized expression of oxidative stress (OS)-related genes identified by trajectory-based differential expression analysis at the spermatogonia phase. These genes are differentially expressed in the stress group. Cells are ordered by pseudotime, with normal cells toward the left and stressed cells toward the right. The arrows indicate the differentiation directions. (D) Twin heatmaps showing normalized expression of OS-related genes identified by trajectory-based differential expression analysis at the meiosis phase. These genes are differentially expressed in the stress group. Cells are ordered by pseudotime, with normal cells toward the left and stressed cells toward the right. The arrows indicate the differentiation directions. (E) The heatmap shows the pairwise comparisons of activities for the selected regulator at the spermatogonia phase. Regulon activities are represented as the scaled AUC scores (area under the recovery curve, defined by SCENIC). (F) The heatmap shows the pairwise comparisons of activities for the selected regulator at the meiosis phase. Regulon activities are represented as the scaled AUC scores (area under the recovery curve, defined by SCENIC).
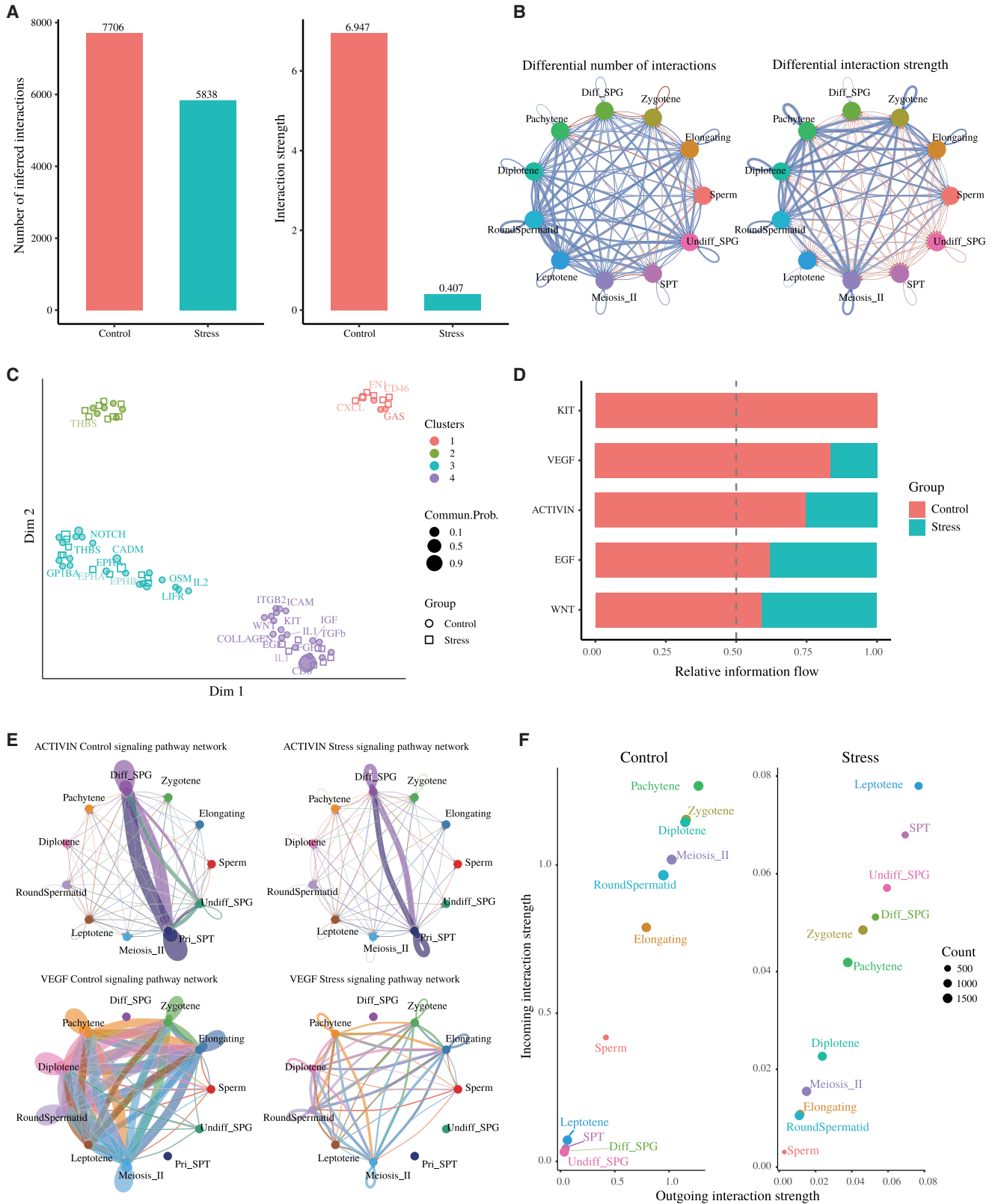
(legend on next page)

(Figure 5B). We then identified differences in signaling pathways enriched for ligand-receptor pairs linking cell interactions between the two groups. We enriched these signals into four clusters according to the functional similarity of signaling pathways (Figure 5C). Notably, activin signaling may help regulate spermatogonia self-renewal and differentiation. Compared with the control group, activin signaling was significantly reduced in the stress group, especially in the interaction between Diff_SPG cells and Pri_SPT cells (Figure 5E). This is consistent with previous work.[40] Additionally, the KIT signaling pathway, which is also known to play a key role in maintaining the balance of spermatogonia self-renewal and differentiation, was significantly reduced in the stress group (Figure 5D). Moreover, VEGF, EGF, WNT, and other pathways were down-regulated in the stress group, and these pathways all contributed to development, proliferation, and differentiation. In particular, the number and strength of interactions between the VEGF signaling pathway and Undiff_SPG with other cells were significantly reduced (Figure 5E). Furthermore, signaling pathways related to the immune system were also altered in the stress group, including a weakening of the CD6 signaling pathway and an enhancement of the complement signaling pathway (Figure S6D).

We also identified cell clusters that varied significantly between the two groups for sending or receiving signals. We found that all cell types in the stress group had significantly lower signal strengths in both sending and receiving. Compared with different cell types in each group, unlike the control group, Undiff_SPG, Diff_SPG, Pri_SPT, and Leptotene cells that were earlier in the spermatogenesis process became the main source of sending and receiving signals in the stress group (Figure 5F). Altogether, these results suggest that psychological stress perturbed the cell-cell interactions between testicular germ cells in a manner detrimental to reproductive development.

DISCUSSION

Male infertility has become a global problem, for which psychological stress has been proven to be an important cause. In this work, we pioneered the study using our previously built rat model to reveal the putative mechanism by which psychological stress causes defective spermatogenesis and reproductive damage (Figure 6). We performed single-cell transcriptome profiling on 11,744 rat testicular cells to provide normal and defective cellular references of spermatogenesis and the potential target genes to explain the etiology of infertility caused by psychological stress. At the cellular level, we revealed major changes during spermatogenesis. We identified six subpopulations of

spermatogonia based on transcriptome profiling, which is consistent with previous reports.[41,42] We found that Pttg1+ spermatogonia (DiSPG.1 cells) and pachytene cells in stressed rats were arrested during differentiation. UnSPG.1 cells are considered to be the origin of the spermatogonia differentiation process,[18,42,43] which is reduced in the stress group. Furthermore, the decrease in UnSPG.1 cells coincided with the increase in UnSPG.2 cells. We speculate that more UnSPG.2 cells failed to progress to a more differentiated state (DiSPG.1 cell).

Furthermore, we found elevated levels of ROS in the testes of rats after psychological stress. Currently, numerous studies have confirmed that small amounts of ROS are essential in the complex process of male germ cell proliferation and maturation.[32,33,44] ROS are involved in the regulation of several fertilization-related physiological responses, including sperm maturation, hyperactivation, capacitation, sperm acrosome reaction, and sperm-oocyte fusion.[32,45–47] However, excessive ROS production may lead to DNA fragmentation, lipid peroxidation, and even cell apoptosis.[32,48,49] All these events can negatively affect sperm quality and male fertility.[50–52] In this work, we found down-regulation of anti-oxidation-related genes and up-regulation of genes promoting ROS generation in the stress group. This may cause OS in rat testes, which further affects spermatogenesis and causes reproductive damage. Specifically, we found that the activity of the ATF2 and RELA regulons was up-regulated in DiSPG.1 cells of the stress group. Among them, the activity of the ATF2 regulator was up-regulated in the stress group, but the expression of ATF2 itself was down-regulated, which may have a specific function. Subsequent Kyoto Encyclopedia of Genes and Genomes (KEGG) enrichment analysis of ATF2-regulated genes in the stress group revealed Oxidative phosphorylation, Chemical carcinogenesis - ROS, and Peroxisome pathways (Figure S6C). Again, this may indicate an elevated level of ROS, which was previously reported to further inhibit the JNK/ATF2 axis, leading to NB4 cells arresting in the G0/G1 phase and undergoing apoptosis.[38]

Moreover, the number and strength of germ cell interactions showed a significant decrease in the stress group. The stress group displays several down-regulated signaling pathways that contribute to development, such as VEGF, EGF, and WNT, which also reveals the detrimental effects of psychological stress on reproductive development.

Overall, we observed retardations for undifferentiated spermatogonium and diplotene differentiation, which affected the course of

Figure 5. Global alterations of the germ cell interactions induced by psychologic stress
(A) Both the CellChat-inferred interaction number (left) and strength (right) between germ cells are attenuated by psychological stress. (B) Circular network diagrams depicting differences in the interaction number (left) or strength (right) in the cell-cell communication network between control and stress groups. Red or blue edges represent increased or decreased signals in the stress group compared with the control group, respectively. (C) Inferred differential signaling networks clustered by functional similarity. Each dot represents the communication network of one signaling pathway. The dot size is proportional to the overall communication probability. Different colors represent different clusters of signaling pathways. Different shapes represent different groups. (D) The representative information flow for the control (red) and stress (cyan) groups. (E) The selected differential signaling networks inferred by CellChat. The edge width represents the communication probability. (F) Psychologic stress significantly altered the sending and receiving of signals for different cell types.
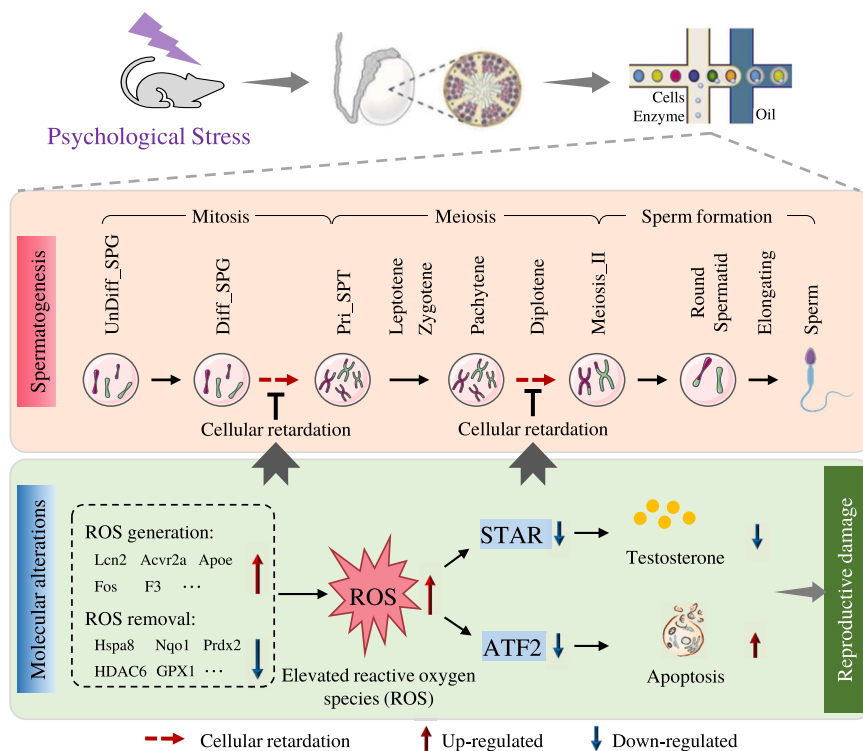
Figure 6. The graphic summary of the putative mechanism by which psychological stress causes disrupted spermatogenesis and male rat reproductive damage

all animal procedures were approved by the Animal Ethics Committee of Xi'an Jiaotong University (No. XJTULAC2022-1151). The detailed procedures and results of the rat model creation are provided in our previous publication.[24]

Histological observation (H&E staining)

First, rat testicular tissues were fixed with paraformaldehyde, dehydrated with ethanol gradient, transparent with xylene, and embedded with liquid paraffin to make paraffin tissue slices. Then, the tissue slices were sectioned using a semi-automatic rotary microtome (Leica, Germany) at approximately 5–7-μm thickness. All tissue slices were further deparaffinized twice with xylene, rehydrated in gradient ethanol (100%, 95%, 90%, 80%), and rinsed in pure water. Then the slices were immersed in hematoxylin for 3–10 min, 1% hydrochloric alcohol differentiation solution for about 5 s, warm water for 10–30 s (until sections turned blue), and soaked in eosin for 1–3 min. Sections were then dehydrated in graded ethanol (80%, 90%, 95%, 100%), cleared with xylene, and sealed with neutral glue. Finally, sectioned tissues were observed under the optical microscope (Nikon light ECLIPSE E200, Japan).

spermatogenesis (Figure 6, top box). We especially hypothesized that psychological stress drives altered expression of genes related to ROS metabolism in the rat testes (Figure 6, bottom box). Specifically, genes related to ROS production are up-regulated, and genes encoding antioxidant proteins are down-regulated. This may lead to excessive ROS levels in rat testes, thereby affecting the expression of key genes such as ATF2 and STAR to cause apoptosis or inhibition of testosterone synthesis. Furthermore, the interactions between rat testicular germ cells were rewired in a manner detrimental to reproductive development after psychological stress.

MATERIALS AND METHODS

Psychologically stressed rat model establishment

Thirty healthy adult male SD rats (280 ± 20 g) were purchased from the Animal Center of Xi'an Jiaotong University (Shaanxi Medical Laboratory Animal Center, China) and were randomly divided into a stress group and a control group (n = 15 per group, three per cage). First, the rats underwent a 7-day acclimation period. Rats were maintained at a constant temperature of 22 ± 2°C and 50% humidity with free access to water and food. The rats in the stress group were subjected to terrified-sound stimulation (45–60 dB, 9:00-12:00 a.m. and 3:00-6:00 p.m.) for 21 consecutive days, and speakers were placed 50 cm on both sides of the cage. Animals in the control group were exposed to the same room conditions but without the terrified-sound stimulus. All experiments were performed following relevant guidelines and regulations, and

Sperm count assay

After the rats were euthanized, the bilateral epididymal tails were harvested to collect sperm fluid. The blood on the surface of the tissues was washed with pre-warmed PBS. Then the tissues were dipped into 1.0 mL of 37°C pre-warmed physiological saline. A small incision was made on the back of the epididymal tails and incubated at 37°C for 30 min. According to the World Health Organization Semen Analysis and Processing Experiment Manual, 4 μL of the sperm suspension at room temperature (25°C) was added to the Makler plate counting area, and individual sperm were counted under optical microscopy.

Singleron Matrix scRNA-seq

Single-cell suspensions were prepared at a concentration of 1×10^5 cells/mL in PBS (HyClone). Single-cell suspensions were then loaded onto microfluidic devices and scRNA-seq libraries were constructed according to Singleron GEXSCOPE protocol by GEXSCOPE Single-Cell RNA Library Kit (Singleron Biotechnologies).[53] Individual libraries were diluted to 4 nM and pooled for sequencing. Pools were sequenced on Illumina NovaSeq with 150 base pair paired-end reads.

The primary analysis of raw read data

Celescope v1.8.1 was used to process the raw reads from scRNA-seq to generate gene expression matrixes. Briefly, raw reads were first processed with fastQC[54] v0.11.4 (https://www.bioinformatics.babraham.ac.uk/projects/fastqc/) and fastp[55] to remove low-quality reads, and with cutadapt[56] to trim poly-A tail and adapter sequences. Cell barcodes and UMI were extracted. After that, we used STAR[57] v2.5.3a to map reads to the reference genome mRatBN6.0 (Ensembl version 104 annotation). The featureCounts[58] v1.6.2 software was used to obtain UMI counts and gene counts per cell and to generate expression matrix files for subsequent analysis.

Quality control, dimension reduction, and clustering

First, cells were filtered by UMI counts below 100,000 and gene counts between 200 and 3,500, followed by removing the cells with over 5% mitochondrial content. After filtering, the functions from Seurat v4.0.4[59] were used for dimension reduction and clustering. We calculated the cell cycle score for each cell using the CellCycleScoring() function. And then we identified anchors using the FindIntegrationAnchors() function, which takes a list of Seurat objects as input and uses these anchors to integrate the six sample datasets of control and stress groups using the IntegrateData() function. Then we used NormalizeData() and ScaleData() functions to normalize and scale all gene expressions and selected the top 3,000 variable genes with FindVariableFeautres() function for PCA analysis. Moreover, the batch effect between samples was removed by Harmony (harmony v0.1.1).[25] Using the top 20 principal components, we separated cells into multiple clusters with FindClusters(). We obtained 15 clusters (Figures S1B–S1D). We then looked at the distribution of each cluster among the six samples (Figure S1F; Table S5). We removed several clusters that existed only in one sample and reclustered the remaining cells. In the end, we obtained 11 cell types, all of which are germ cells: Undifferentiated spermatogonia (Undiff_SPG), differentiated spermatogonia (Diff_SPG), primary spermatocytes (Pri_SPT), leptotene, zygotene, pachytene, diplotene, second secondary meiotic cells (Meiosis_II), round sperm cells (RoundSpermatid), elongated sperm cells (Elongating), Sperm cells. Finally, the UMAP algorithm was applied to visualize cells in a two-dimensional space.

DEGs analysis

To identify marker genes for each cell cluster, we used the Seurat FindMarkers() function based on the Wilcox likelihood-ratio test with default parameters and selected the genes expressed in more than 10% of the cells in a cluster and with an average log2(Fold Change) value greater than 0.25 as marker genes. For the cell type annotation of each cluster, we combined the discovered marker genes with knowledge from the literature and displayed the expression of markers of each cell type with heatmaps, dotplots, and violinplots that were generated with the Seurat DoHeatmap, DotPlot, and Vlnplot functions.

To identify DEGs across groups of cell types, we utilized the DESeq2 (v1.38.3)[60] tool to perform pseudobulk differential expression anal-

ysis on each cell type. Taking the cell group as the unit, for each cell group, the average expression level of the gene in each sample was taken as the expression level of the gene, that is, the sum of the UMI counts of all cells in the cell group was divided by the number of cells with non-zero counts. A total of six samples from the stress group and the control group were used for gene differential expression analysis using DESeq2,[60] and selected its p value less than 0.05 and the log2(Fold Change) value greater than 1.0 as DEGs.

Pathway enrichment analysis

To investigate the potential functions of DEGs, GO and KEGG analyses were used with the "clusterProfiler (v4.7.1.003)" R package.[61] Pathways with a p value less than 0.05 were considered significantly enriched. GO gene sets, including molecular function, biological process, and cellular component categories, were used as references.

RNA velocity estimation and embedding

RNA velocity analysis was performed using scVelo (v0.2.4) to estimate RNA velocity to study cellular dynamics[62] and infer a potential time to reconstruct the time series of transcriptomic events. RNA velocity is the temporal derivative of measured mRNA abundance (mature spliced/nascent unspliced transcripts), allowing an estimate of each cell's future developmental direction. Abundance estimates for each sample were combined with the loompy (v3.0.6) package, similar to the scheme in the Seurat integration step, and merge the merged abundance data with the PAGA anndata object using scVelo. Abundance estimates are normalized and filtered while requiring a minimum abundance of 10 per gene in spliced and unspliced counts. We computed the first and second moments using the first 30 PCs and 30 neighbors in the neighborhood graph, and applied a likelihood-based kinetic model from scVelo to recover the full splicing dynamics before estimating velocity. In addition to velocity maps and projections of velocity to UMAP embeddings, latent time for gene sharing was calculated. The latent time is entirely based on transcriptional dynamics and represents the cell's internal clock. For latent time calculations, cells from the most undifferentiated cell type were used as root cells.

Trajectory-based differential expression analysis

Monocle2 (v2.26.0) was used to reconstruct the cell differentiation trajectory.[63] DEGs were used to sort cells in order of spatial-temporal differentiation. We used DDRTree to perform FindVairableFeatures() and dimension reduction. Then, the trajectory was visualized by the plot_cell_trajectory() function. Cells were arranged along the order of differentiation, and we used the plot_genes_branched_heatmap() function to create a heatmap showing the difference in gene expression along the differentiation process between the control and stress groups.

Rat-to-human homologous gene conversion

We used the R package biomaRt (v2.48.3) to perform homology mapping of rat gene IDs to human genes. The bioMart database is a gene conversion tool owned by Ensembl. By linking the bioMart database, we mapped 21,170 rat genes to their human orthologues. After

removing deletions and duplications, we finally obtained 14,993 human homologous genes.

Cell-cell communication analysis

We used CellChat (v1.6.1)[64] to infer the role of intercellular communication. Since CellChat does not currently support rat species, it is necessary to perform homologous conversion to convert rat genes into human homologous genes. CellChat objects are created via CellChat (https://github.com/sqjin/CellChat, R package, v.1) based on the UMI count matrix for each group (Control, Stress). Set "Cell-ChatDB.human" as the ligand-receptor interaction database, and then perform cell-cell communication analysis with default settings. Merge the CellChat objects of each group by the function mergeCellChat to get a comparison of the total number of interactions and the strength of the interactions. The visualization of the number of differences or the strength of interactions between different cell populations is achieved by the function netVisual_diffInteraction. Finally, differentially expressed signaling pathways were discovered through the function rankNet, and the distribution of signaling gene expression between different datasets was visualized through the function plotGeneExpression.

Gene regulatory network inference

The Python version of the SCENIC pipeline (pyscenic, version 0.11.0) was used for gene regulatory network inference.[65] We performed the analysis by following the protocol steps described in the SCENIC workflow.[66] Since SCENIC does not currently support rat species, it is necessary to perform homologous conversion to convert rat genes into human homologous genes. SCENIC uses standard normalized UMI counts with the GRNBoost2 algorithm[67] to identify paired genes and co-expressed TFs. Furthermore, based on the human motif v9 and hg38 databases from cisTargetDB, we pruned the co-expression modules derived from this analysis to remove indirect targets and false positives. We refer to modules with significant motif enrichment of the correct upstream regulator as regulons. Cells with enriched expression for genes in a regulon were marked as active for the particular regulon.

Briefly, the "pyscenic grn" function was first used to generate co-expression gene regulatory networks using the "grnboost2" method. The AUCell analysis was further performed to quantify the activity of gene signatures in single cells using the "pyscenic aucell" function with parameters "rank_threshold" 5000, "auc_threshold" 0.05, and "nes_threshold" 3.

Statistical analysis

We identified DEGs between two groups and cell types using a Wilcoxon Rank-Sum test. The significance of differences was determined as indicated, and differences with $p < 0.05$ were considered statistically significant.

DATA AND CODE AVAILABILITY

Single-cell RNA sequencing data are deposited at the NIH Gene Expression Omnibus with the access ID GEO: GSE233950. All codes and source data for reproducing the results are available at figShare: https://figshare.com/s/2b1ffa0d0edafff5a807. All software and tools are listed in Table S6.

SUPPLEMENTAL INFORMATION

Supplemental information can be found online at https://doi.org/10.1016/j.omtn.2024.102158.

AUTHOR CONTRIBUTIONS

J.Y., Y.G.X., and R.F.L. conceived and designed the study. R.F.L. and Y.F.D. performed the bioinformatics analysis and interpreted the results. R.F.L. and Y.F.D. contributed equally to this work. K.L., X.F.X., L.Y.Z., C.G., S.F.G., and Y.F.Y. conducted animal model construction and experimental analysis. All authors contributed to the writing and provided comments on the paper. All authors read and approved the final manuscript.

DECLARATION OF INTERESTS

The authors declare no competing interests.

REFERENCES

1. Krausz, C., and Riera-Escamilla, A. (2018). Genetics of male infertility. Nat. Rev. Urol. 15, 369–384.

2. Agarwal, A., Baskaran, S., Parekh, N., Cho, C.L., Henkel, R., Vij, S., Arafa, M., Panner Selvam, M.K., and Shah, R. (2021). Male infertility. Lancet 397, 319–333.

3. Hackett, R.A., and Steptoe, A. (2017). Type 2 diabetes mellitus and psychological stress - a modifiable risk factor. Nat. Rev. Endocrinol. 13, 547–560.

4. Bräuner, E.V., Nordkap, L., Priskorn, L., Hansen, Å.M., Bang, A.K., Holmboe, S.A., Schmidt, L., Jensen, T.K., and Jørgensen, N. (2020). Psychological stress, stressful life events, male factor infertility, and testicular function: a cross-sectional study. Fertil. Steril. 113, 865–875.

5. Nargund, V.H. (2015). Effects of psychological stress on male fertility. Nat. Rev. Urol. 12, 373–382.

6. Basu, S. (2014). Psychological stress and male infertility. Male Infertility, 141–159. Springer.

7. Ilacqua, A., Izzo, G., Emerenziani, G.P., Baldari, C., and Aversa, A. (2018). Lifestyle and fertility: the influence of stress and quality of life on male fertility. Reprod. Biol. Endocrinol. 16, 115.

8. Juárez-Rojas, L., Vigueras-Villaseñor, R.M., Casillas, F., and Retana-Márquez, S. (2017). Gradual decrease in spermatogenesis caused by chronic stress. Acta Histochem. 119, 284–291.

9. Bhongade, M.B., Prasad, S., Jiloha, R.C., Ray, P.C., Mohapatra, S., and Koner, B.C. (2015). Effect of psychological stress on fertility hormones and seminal quality in male partners of infertile couples. Andrologia 47, 336–342.

10. Toufexis, D., Rivarola, M.A., Lara, H., and Viau, V. (2014). Stress and the Reproductive Axis. J. Neuroendocrinol. 26, 573–586.

11. Gollenberg, A.L., Liu, F., Brazil, C., Drobnis, E.Z., Guzick, D., Overstreet, J.W., Redmon, J.B., Sparks, A., Wang, C., and Swan, S.H. (2010). Semen quality in fertile men in relation to psychosocial stress. Fertil. Steril. 93, 1104–1111.

12. Collodel, G., Moretti, E., Fontani, V., Rinaldi, S., Aravagli, L., Saragò, G., Capitani, S., and Anichini, C. (2008). Effect of emotional stress on sperm quality. Indian J. Med. Res. 128, 254–261.

13. Wingfield, J.C., and Sapolsky, R.M. (2003). Reproduction and resistance to stress: When and how. J. Neuroendocrinol. 15, 711–724.

14. Tang, F., Barbacioru, C., Wang, Y., Nordman, E., Lee, C., Xu, N., Wang, X., Bodeau, J., Tuch, B.B., Siddiqui, A., et al. (2009). mRNA-Seq whole-transcriptome analysis of a single cell. Nat. Methods 6, 377–382.

15. Saliba, A.E., Westermann, A.J., Gorski, S.A., and Vogel, J. (2014). Single-cell RNA-seq: advances and future challenges. Nucleic Acids Res. 42, 8845–8860.

16. Chen, Y., Zheng, Y., Gao, Y., Lin, Z., Yang, S., Wang, T., Wang, Q., Xie, N., Hua, R., Liu, M., et al. (2018). Single-cell RNA-seq uncovers dynamic processes and critical regulators in mouse spermatogenesis. Cell Res. 28, 879–896.

17. Wang, M., Liu, X., Chang, G., Chen, Y., An, G., Yan, L., Gao, S., Xu, Y., Cui, Y., Dong, J., et al. (2018). Single-Cell RNA Sequencing Analysis Reveals Sequential Cell Fate Transition during Human Spermatogenesis. Cell Stem Cell 23, 599–614.e4.

18. Shami, A.N., Zheng, X., Munyoki, S.K., Ma, Q., Manske, G.L., Green, C.D., Sukhwani, M., Orwig, K.E., Li, J.Z., and Hammoud, S.S. (2020). Single-Cell RNA Sequencing of Human, Macaque, and Mouse Testes Uncovers Conserved and Divergent Features of Mammalian Spermatogenesis. Dev. Cell 54, 529–547.e12.

19. Lukassen, S., Bosch, E., Ekici, A.B., and Winterpacht, A. (2018). Characterization of germ cell differentiation in the male mouse through single-cell RNA sequencing. Sci. Rep. 8, 6521.

20. Green, C.D., Ma, Q., Manske, G.L., Shami, A.N., Zheng, X., Marini, S., Moritz, L., Sultan, C., Gurczynski, S.J., Moore, B.B., et al. (2018). A Comprehensive Roadmap of Murine Spermatogenesis Defined by Single-Cell RNA-Seq. Dev. Cell 46, 651–667.e10.

21. Priya, P.H., and Reddy, P.S. (2012). Effect of Restraint Stress on Lead-Induced Male Reproductive Toxicity in Rats. J. Exp. Zool. Part A 317, 455–465.

22. Fenchel, D., Levkovitz, Y., Vainer, E., Kaplan, Z., Zohar, J., and Cohen, H. (2015). Beyond the HPA-axis: The role of the gonadal steroid hormone receptors in modulating stress-related responses in an animal model of PTSD. Eur. Neuropsychopharmacol. 25, 944–957.

23. Nirupama, M., Devaki, M., Nirupama, R., and Yajurvedi, H.N. (2013). Chronic intermittent stress-induced alterations in the spermatogenesis and antioxidant status of the testis are irreversible in albino rat. J. Physiol. Biochem. 69, 59–68.

24. Xiong, X., Zhang, L., Fan, M., Han, L., Wu, Q., Liu, S., Miao, J., Liu, L., Wang, X., Guo, B., et al. (2019). β-Endorphin induction by psychological stress promotes Leydig cell apoptosis through p38 MAPK pathway in male rats. Cells 8, 1265.

25. Korsunsky, I., Millard, N., Fan, J., Slowikowski, K., Zhang, F., Wei, K., Baglaenko, Y., Brenner, M., Loh, P.R., and Raychaudhuri, S. (2019). Fast, sensitive and accurate integration of single-cell data with Harmony. Nat. Methods 16, 1289–1296.

26. Vertika, S., Singh, K.K., and Rajender, S. (2020). Mitochondria, spermatogenesis, and male infertility - An update. Mitochondrion 54, 26–40.

27. Lee, J.P.W., Foote, A., Fan, H., Peral de Castro, C., Lang, T., Jones, S.A., Gavrilescu, N., Mills, K.H.G., Leech, M., Morand, E.F., and Harris, J. (2016). Loss of autophagy enhances MIF/macrophage migration inhibitory factor release by macrophages. Autophagy 12, 907–916.

28. Zhang, J.Q., Ren, Q.L., Chen, J.F., Lv, L.Y., Wang, J., Shen, M., Xing, B.S., and Wang, X.W. (2022). Downregulation of miR-192 Alleviates Oxidative Stress-Induced Porcine Granulosa Cell Injury by Directly Targeting Acvr2a. Cells 11.

29. Guo, Z., Wang, G., Wu, B., Chou, W.C., Cheng, L., Zhou, C., Lou, J., Wu, D., Su, L., Zheng, J., et al. (2020). DCAF1 regulates Treg senescence via the ROS axis during immunological aging. J. Clin. Invest. 130, 5893–5908.

30. Guo, H., Ouyang, Y., Yin, H., Cui, H., Deng, H., Liu, H., Jian, Z., Fang, J., Zuo, Z., Wang, X., et al. (2022). Induction of autophagy via the ROS-dependent AMPK-

mTOR pathway protects copper-induced spermatogenesis disorder. Redox Biol. 49, 102227.

31. Song, J., Gao, X., Tang, Z., Li, H., Ruan, Y., Liu, Z., Wang, T., Wang, S., Liu, J., and Jiang, H. (2020). Protective effect of Berberine on reproductive function and spermatogenesis in diabetic rats via inhibition of ROS/JAK2/NF kappa B pathway. Andrology 8, 793–806.

32. Takeshima, T., Usui, K., Mori, K., Asai, T., Yasuda, K., Kuroda, S., and Yumura, Y. (2021). Oxidative stress and male infertility. Reprod. Med. Biol. 20, 41–52.

33. Guerriero, G., Trocchia, S., Abdel-Gawad, F.K., and Ciarcia, G. (2014). Roles of reactive oxygen species in the spermatogenesis regulation. Front. Endocrinol. 5, 56.

34. Leng, Y., Wu, Y., Lei, S.Q., Zhou, B., Qiu, Z., Wang, K., and Xia, Z.Y. (2018). Inhibition of HDAC6 Activity Alleviates Myocardial Ischemia/Reperfusion Injury in Diabetic Rats: Potential Role of Peroxiredoxin 1 Acetylation and Redox Regulation. Oxid. Med. Cell. Longev. 2018, 9494052.

35. Liu, S., Tang, Y., Chen, B., Zhao, Y., Aguilar, Z.P., Tao, X., and Xu, H. (2021). Inhibition of testosterone synthesis induced by oral TiO2 NPs is associated with ROS-MAPK(ERK1/2)-StAR signaling pathway in SD rat. Toxicol. Res. 10, 937–946.

36. Ba, X., Gupta, S., Davidson, M., and Garg, N.J. (2010). Trypanosoma cruzi Induces the Reactive Oxygen Species-PARP-1-RelA Pathway for Up-regulation of Cytokine Expression in Cardiomyocytes. J. Biol. Chem. 285, 11596–11606.

37. Luo, Y., Yu, M.H., Yan, Y.R., Zhou, Y., Qin, S.L., Huang, Y.Z., Qin, J., and Zhong, M. (2020). Rab27A promotes cellular apoptosis and ROS production by regulating the miRNA-124-3p/STAT3/RelA signalling pathway in ulcerative colitis. J. Cell Mol. Med. 24, 11330–11342.

38. An, J.J., Shi, K.J., Wei, W., Hua, F.Y., Ci, Y.L., Jiang, Q., Li, F., Wu, P., Hui, K.Y., Yang, Y., and Xu, C.M. (2013). The ROS/JNK/ATF2 pathway mediates selenite-induced leukemia NB4 cell cycle arrest and apoptosis in vitro and in vivo. Cell Death Dis. 4, e973.

39. Sharpe, R.M., Maddocks, S., and Kerr, J.B. (1990). Cell-Cell Interactions in the Control of Spermatogenesis as Studied Using Leydig-Cell Destruction and Testosterone Replacement. Am. J. Anat. 188, 3–20.

40. Guo, J., Nie, X., Giebler, M., Mlcochova, H., Wang, Y., Grow, E.J., DonorConnect, Kim, R., Tharmalingam, M., Matilionyte, G., et al. (2020). The Dynamic Transcriptional Cell Atlas of Testis Development during Human Puberty. Cell Stem Cell 26, 262–276.e4.

41. Sohni, A., Tan, K., Song, H.W., Burow, D., de Rooij, D.G., Laurent, L., Hsieh, T.C., Rabah, R., Hammoud, S.S., Vicini, E., and Wilkinson, M.F. (2019). The Neonatal and Adult Human Testis Defined at the Single-Cell Level. Cell Rep. 26, 1501–1517.e4.

42. Di Persio, S., Tekath, T., Siebert-Kuss, L.M., Cremers, J.F., Wistuba, J., Li, X., Meyer Zu Hörste, G., Drexler, H.C.A., Wyrwoll, M.J., Tüttelmann, F., et al. (2021). Single-cell RNA-seq unravels alterations of the human spermatogonial stem cell compartment in patients with impaired spermatogenesis. Cell Rep. Med. 2, 100395.

43. Guo, J., Grow, E.J., Mlcochova, H., Maher, G.J., Lindskog, C., Nie, X., Guo, Y., Takei, Y., Yun, J., Cai, L., et al. (2018). The adult human testis transcriptional cell atlas. Cell Res. 28, 1141–1157.

44. Song, J., Gao, X., Tang, Z., Li, H., Ruan, Y., Liu, Z., Wang, T., Wang, S., Liu, J., and Jiang, H. (2020). Protective effect of Berberine on reproductive function and spermatogenesis in diabetic rats via inhibition of ROS/JAK2/NFkappaB pathway. Andrology 8, 793–806.

45. Upadhyay, V.R., Ramesh, V., Dewry, R.K., Yadav, D.K., and Ponraj, P. (2022). Bimodal interplay of reactive oxygen and nitrogen species in physiology and pathophysiology of bovine sperm function. Theriogenology 187, 82–94.

46. Blondin, P., Coenen, K., and Sirard, M.A. (1997). The impact of reactive oxygen species on bovine sperm fertilizing ability and oocyte maturation. J. Androl. 18, 454–460.

47. Du Plessis, S.S., Agarwal, A., Halabi, J., and Tvrda, E. (2015). Contemporary evidence on the physiological role of reactive oxygen species in human sperm function. J. Assist. Reprod. Genet. 32, 509–520.

48. Chen, C., Ouyang, W., Grigura, V., Zhou, Q., Carnes, K., Lim, H., Zhao, G.Q., Arber, S., Kurpios, N., Murphy, T.L., et al. (2005). ERM is required for transcriptional control of the spermatogonial stem cell niche. Nature 436, 1030–1034.

49. Ranawat, P., and Bansal, M.P. (2009). Apoptosis induced by modulation in selenium status involves p38 MAPK and ROS: implications in spermatogenesis. Mol. Cell. Biochem. 330, 83–95.

50. Agarwal, A., Sharma, R.K., Sharma, R., Assidi, M., Abuzenadah, A.M., Alshahrani, S., Durairajanayagam, D., and Sabanegh, E. (2014). Characterizing semen parameters and their association with reactive oxygen species in infertile men. Reprod. Biol. Endocrinol. 12, 33.

51. Aziz, N., Saleh, R.A., Sharma, R.K., Lewis-Jones, I., Esfandiari, N., Thomas, A.J., and Agarwal, A. (2004). Novel association between sperm reactive oxygen species production, sperm morphological defects, and the sperm deformity index. Fertil. Steril. 81, 349–354.

52. Agarwal, A., Tvrda, E., and Sharma, R. (2014). Relationship amongst teratozoospermia, seminal oxidative stress and male infertility. Reprod. Biol. Endocrinol. 12, 45.

53. Dura, B., Choi, J.Y., Zhang, K., Damsky, W., Thakral, D., Bosenberg, M., Craft, J., and Fan, R. (2019). scFTD-seq: freeze-thaw lysis based, portable approach toward highly distributed single-cell 3 mRNA profiling. Nucleic Acids Res. 47, e16.

54. Andrews, S. (2010). FastQC: A Quality Control Tool for High Throughput Sequence Data (Babraham Bioinformatics, Babraham Institute).

55. Chen, S., Zhou, Y., Chen, Y., and Gu, J. (2018). fastp: an ultra-fast all-in-one FASTQ preprocessor. Bioinformatics 34, 884–890.

56. Martin, M. (2011). Cutadapt removes adapter sequences from high-throughput sequencing reads. EMBnet. j. 17, 10–12.

57. Dobin, A., Davis, C.A., Schlesinger, F., Drenkow, J., Zaleski, C., Jha, S., Batut, P., Chaisson, M., and Gingeras, T.R. (2013). STAR: ultrafast universal RNA-seq aligner. Bioinformatics 29, 15–21.

58. Liao, Y., Smyth, G.K., and Shi, W. (2014). featureCounts: an efficient general purpose program for assigning sequence reads to genomic features. Bioinformatics 30, 923–930.

59. Satija, R., Farrell, J.A., Gennert, D., Schier, A.F., and Regev, A. (2015). Spatial reconstruction of single-cell gene expression data. Nat. Biotechnol. 33, 495–502.

60. Love, M.I., Huber, W., and Anders, S. (2014). Moderated estimation of fold change and dispersion for RNA-seq data with DESeq2. Genome Biol. 15, 550.

61. Yu, G., Wang, L.G., Han, Y., and He, Q.Y. (2012). clusterProfiler: an R Package for Comparing Biological Themes Among Gene Clusters. OMICS 16, 284–287.

62. Bergen, V., Lange, M., Peidli, S., Wolf, F.A., and Theis, F.J. (2020). Generalizing RNA velocity to transient cell states through dynamical modeling. Nat. Biotechnol. 38, 1408–1414.

63. Qiu, X., Hill, A., Packer, J., Lin, D., Ma, Y.A., and Trapnell, C. (2017). Single-cell mRNA quantification and differential analysis with Census. Nat. Methods 14, 309–315.

64. Jin, S., Guerrero-Juarez, C.F., Zhang, L., Chang, I., Ramos, R., Kuan, C.H., Myung, P., Plikus, M.V., and Nie, Q. (2021). Inference and analysis of cell-cell communication using CellChat. Nat. Commun. 12, 1088.

65. van de Sande, B., Flerin, C., Davie, K., De Waegeneer, M., Hulselmans, G., Aibar, S., Seurinck, R., Saelens, W., Cannoodt, R., Rouchon, Q., et al. (2020). A scalable SCENIC workflow for single-cell gene regulatory network analysis. Nat. Protoc. 15, 2247–2276.

66. Aibar, S., González-Blas, C.B., Moerman, T., Huynh-Thu, V.A., Imrichova, H., Hulselmans, G., Rambow, F., Marine, J.C., Geurts, P., Aerts, J., et al. (2017). SCENIC: single-cell regulatory network inference and clustering. Nat. Methods 14, 1083–1086.

67. Moerman, T., Aibar Santos, S., Bravo González-Blas, C., Simm, J., Moreau, Y., Aerts, J., and Aerts, S. (2019). GRNBoost2 and Arboreto: efficient and scalable inference of gene regulatory networks. Bioinformatics 35, 2159–2161.